EARLY STAGES OF THE BLOODY FROGFISH, *ANTENNARIUS SANGUINEUS* GILL 1863, AND THE BANDTAIL FROGFISH, *ANTENNATUS STRIGATUS* (GILL 1863) (PISCES: ANTENNARIIDAE)

WILLIAM WATSON
National Marine Fisheries Service
Southwest Fisheries Science Center
P.O. Box 271
La Jolla, California 92038-0271
billwatson@ucsd.edu

ABSTRACT

Antennarius sanguineus and *Antennatus strigatus* are benthic residents of coastal waters from the lower Gulf of California to northern Chile and Ecuador, respectively. Planktonic larvae of both species, collected primarily from the lower Gulf of California, are deep-bodied and compressed with large head, moderately long preanal length, and inflated skin. *Antennarius sanguineus* undergoes notochord flexion at 2.6–2.9 mm through 2.9–3.2 mm and settles from the plankton at about 8.0–8.5 mm; *Antennatus strigatus* completes flexion before 2.3 mm and settles at an unknown size <11 mm. Shortly before settlement small dermal spinules enclosed in small fleshy papillae begin to form in *Antennarius sanguineus*; larger, bare spinules are already present in the smallest available specimen (2.3 mm) of *Antennatus strigatus*. Caudal and dorsal fin rays are first to begin developing during the preflexion stage in *Antennarius sanguineus*, followed by anal, pectoral, and pelvic fin rays during the flexion stage. Neural and haemal arches and vertebral centra begin to ossify during the preflexion stage; addition of elements apparently is anterior to posterior. Ossification of the skull is already well under way in the smallest cleared and stained specimen of *A. sanguineus* (2.9 mm, preflexion stage).

Larval *A. sanguineus* are pigmented primarily on the mid- and hindbrain, on the opercle during the latter part of development, internally on the trunk, dorsally and laterally on the gut, and internally on the tail. Larval *Antennatus strigatus* are pigmented primarily on the lower jaw, laterally and ventrally on the cranium, on the opercular area, dorsally and laterally on the gut, and internally around the vertebral column of the trunk and much of the tail.

Larval *Antennarius avalonis*, *A. sanguineus*, and *Antennatus strigatus* can be distinguished by modal fin-ray counts and by pigment patterns. Diagnostic pigment includes (1) the internal dorsal melanophore series extending posteriorly from the nape, and in late larvae the external melanophores on the head and gut in *Antennarius avalonis*; (2) the mid-tail bar of melanophores in *A. sanguineus*; and (3) the jaw pigment and internal melanophores above and below the vertebral column in *Antennatus strigatus*.

Antennarius avalonis has a specialized postflexion larval stage (the scutatus) that the others lack.

INTRODUCTION

Three frogfish species—*Antennarius avalonis*, *A. sanguineus*, and *Antennatus strigatus*—occur in the California Current vicinity (Pietsch and Grobecker 1987; Schneider and Lavenberg 1995). All three are benthic residents of coastal waters; *Antennarius sanguineus* and *Antennatus strigatus* are shallow-living (< ca. 40 m depth, most commonly < ca. 15 m), while *Antennarius avalonis* ranges deeper (to ca. 300 m, usually <100 m). Larvae of all three species have been collected primarily from the Gulf of California and Pacific coast of mainland Mexico and Central America; a few larval *A. avalonis* and two *A. sanguineus* were taken in CalCOFI collections off the Pacific coast of southern Baja California Sur.

Larval *A. avalonis* were described by Watson (1996), but early development stages of *A. sanguineus* and *Antennatus strigatus* have not been described. The purposes of this paper are to document the early development of *Antennarius sanguineus* and *Antennatus strigatus* from planktonic larval to early benthic juvenile stage, and to provide characters for distinguishing the larvae of all three species in plankton collections. Owing to the small number of specimens available, the description of *A. strigatus* is largely limited to illustrations and comparisons with the *Antennarius* species.

METHODS

Descriptions are based on 13 planktonic larvae and 35 benthic juveniles of *Antennarius sanguineus*, and 4 planktonic larvae and 6 benthic juveniles of *Antennatus strigatus* (Appendix). Eleven of the larval *Antennarius sanguineus* and three of the larval *Antennatus strigatus* were obtained from plankton collections taken with standard CalCOFI techniques (Kramer et al. 1972; Moser et al. 1974, 1994). The remaining two larval *Antennarius sanguineus* were obtained from plankton collections made during Scripps Institution of Oceanography (SIO) expedition Scot (SIO 1965), and one larval *Antennatus strigatus* was collected during Inter-American Tropical Tuna Commission (IATTC) survey 90048. All benthic juveniles were obtained from the SIO Marine Vertebrates Collection. Comparisons with *Antennarius avalonis* are

based on Watson (1996) and on five additional post-flexion specimens taken during CalCOFI and IATTC surveys (Appendix).

All specimens were used for the description of pigmentation (melanistic pigment only). Twenty-three of the *A. sanguineus* (all larvae and ten juveniles) were included in measurement series. Dimensions measured, including body length, preanal length, head length, snout length, eye diameter, head width, body depth, and lengths of the pectoral and pelvic fins, are defined by Moser (1996). Larval lengths always refer to body length. Head width includes the inflated skin; body depth was measured inclusive (BD) and exclusive (BDi) of the inflated skin. Measurements were made to the nearest 0.04 mm with a Wild M-5 binocular microscope equipped with an ocular micrometer. Illustrations were made with the same microscope equipped with a camera lucida.

Five larval *Antennarius sanguineus* (2.9–8.1 mm) and one larval *A. avalonis* (5.3 mm) were cleared and stained with alcian blue and alizarin red S following the method of Taylor and Van Dyke (1985) to help determine the sequence of fin formation and to make a cursory examination of skeletal development. Staining was not entirely successful, perhaps owing to the nearly 40 years (or more) of formalin storage of the larvae used (although the oldest specimen stained well—after 46 years of storage). Even when poorly stained, the bony structures could often be recognized by their hyaline appearance, and the cartilaginous structures by their reticulated appearance.

DESCRIPTION

Antennarius sanguineus Gill 1863 Bloody Frogfish

Morphology. *Antennarius sanguineus* is deep-bodied and somewhat compressed, with a large head, moderately long preanal length, and inflated skin throughout larval development (table 1; figs. 1 and 2). Relative head and snout lengths change little during development, whereas relative eye diameter remains stable through the larval period, then decreases after settlement (table 1). The other proportions gradually increase through the postflexion stage, then stabilize (preanal length), continue to increase (fin lengths), or decrease (body depth, head width). The decrease in relative body depth coincides with deflation of the skin at settlement; body depth exclusive of the inflated skin continues to increase relative to body length (table 1).

The only preflexion-stage specimen available (2.9 mm) has a thin, transparent, mildly inflated skin; short, tubular anterior nostrils; a moderately small, somewhat oblique mouth opening; a coiled gut; and developing rays in the dorsal and caudal fins (fig. 1a). No gas bladder is visible. Notochord flexion begins between ca. 2.6 and 2.9 mm and is completed between between ca. 2.9 and 3.6

TABLE 1

Summary of Measurements of *Antennarius sanguineus*, Expressed as Percentage of Body Length (BL) or Head Length (HL); for Each Measurement the Range Is Given Above and the Mean Is Given Below

	Planktonic stage			Benthic juvenile stage
	Preflexion	Flexion	Postflexion	
Number of specimens	1	4	8	10
Size range (mm)	2.9	2.6–3.2	2.9–8.4	8.1–23.9
Proportions[a]				
Sn-A/BL	52	59–68	69–74	63–74
		64	71	71
BDi/BL	33	39–43	42–63	48–64
		41	54	57
BD/BL	37	43–54	50–72	49–66
		50	62	58
HL/BL	33	36–45	37–44	35–48
		41	41	41
P1L/BL	10	9–12	13–26	20–26
		11	21	23
P2L/BL	0	0–1	0–15	17–21
		1	9	18
HW/HL	94	56–72	79–134	82–112
		66	104	94
SnL/HL	19	12–21	12–20	14–20
		17	16	17
ED/HL	38	37–38	34–44	25–31
		37	38	28

[a]Measurements include preanal length (Sn-A), body depth inclusive (BD) and exclusive (BDi) of the inflated skin, head length (HL), pectoral fin length (P1L), pelvic fin length (P2L), head width (HW), snout length (SnL) and eye diameter (ED).

mm (fig. 1b, c). Settlement and transformation to the benthic juvenile stage occurs between about 8.0 and 8.5 mm. During notochord flexion the skin tends to become more inflated, but it remains thin and translucent until midway through the postflexion stage, when it begins to thicken and become increasingly opaque (fig. 2a). Shortly before settlement a row of widely spaced, small, fleshy papillae forms anteriorly on the head and dorsolaterally along each side of the trunk. A small dermal spinule consisting of a horseshoe-shaped to ring-like base bearing two small spines is enclosed in each papilla. At settlement the skin nearly completely deflates and the papillae rapidly increase in number (fig. 2b), especially ventrally on the head at first, then spreading dorsad and caudad to densely cover the body and proximal parts of the fins by ca. 9.5 mm. The spinules are partially exposed by this size. The tubular anterior nostrils elongate and become prominent during the postflexion stage. The mouth opening remains oblique through early postflexion stage, then gradually rotates upward to become nearly vertical by settlement.

Fin and skeletal development. The sequence of initial fin-ray formation could not be determined except that the dorsal soft rays and caudal rays are first to begin forming: the anterior 8 dorsal rays and 7 (3+4) of the 9 caudal rays are forming in the preflexion specimen. Addition
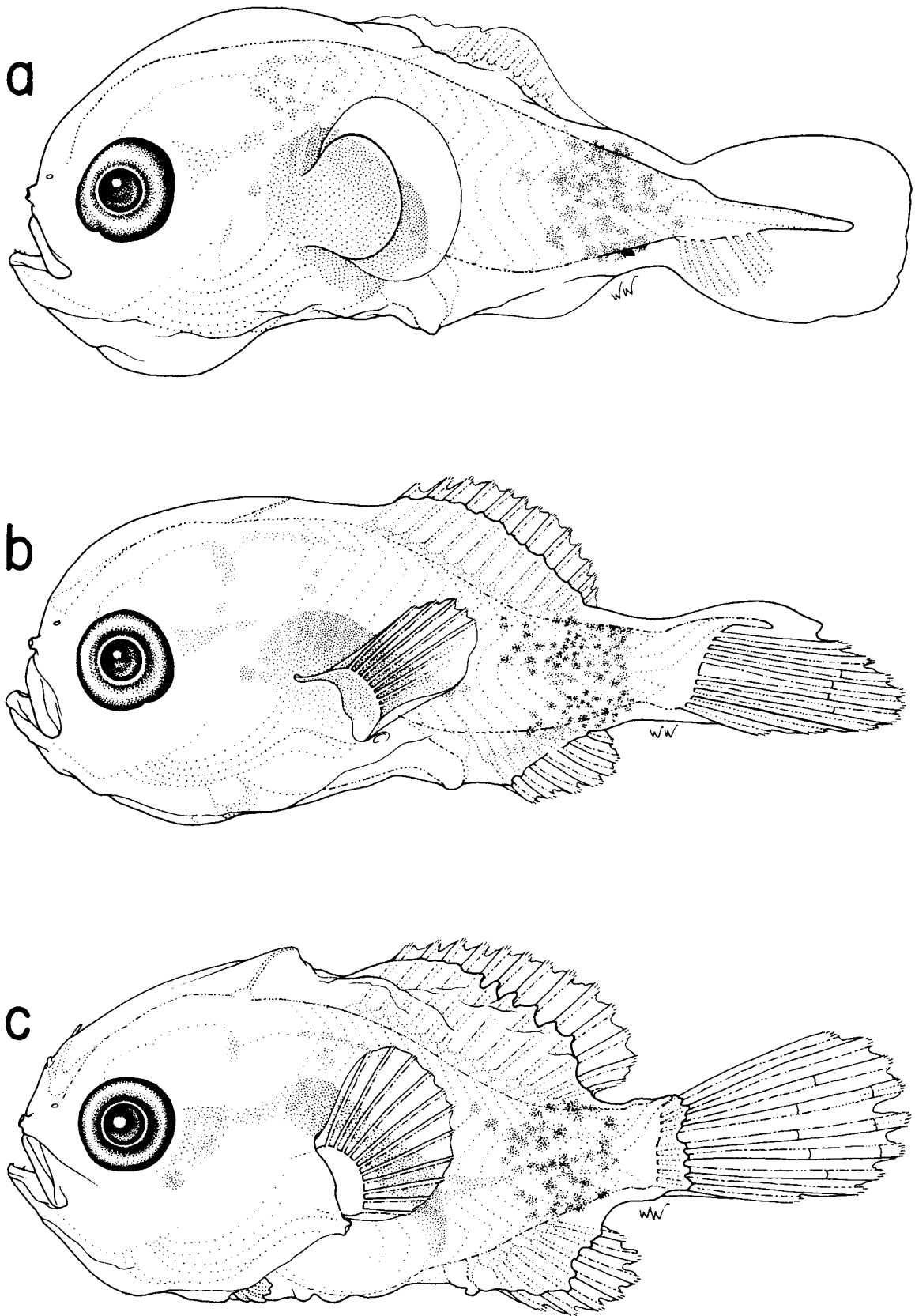
Figure 1. *Antennarius sanguineus: a*, preflexion, 2.9 mm (CalCOFI 5209, station 153G.32); *b*, flexion, 3.2 mm (CalCOFI 5612, station 173G.10); *c*, postflexion, 3.6 mm (CalCOFI 5706, station 153.20).
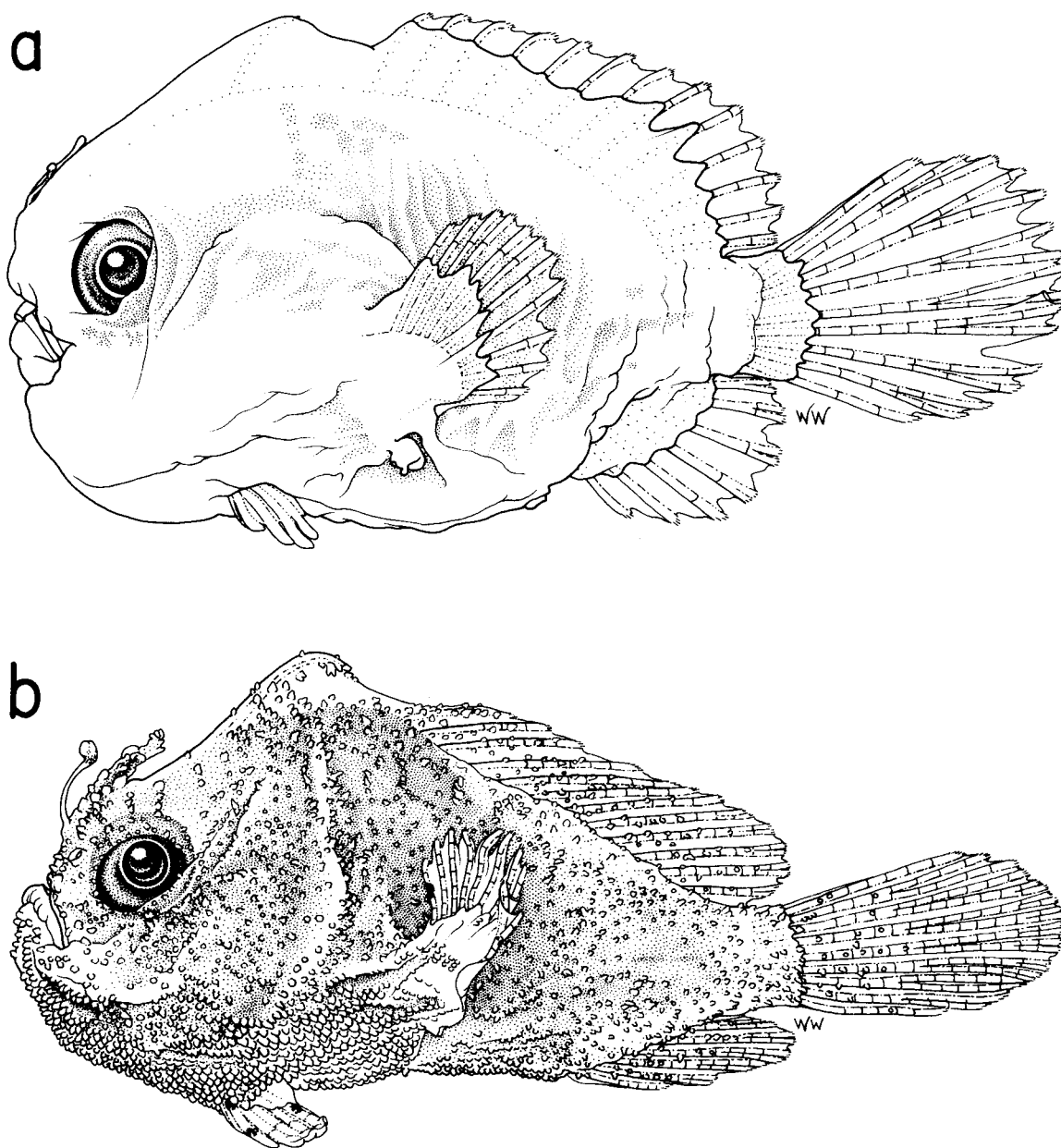
Figure 2.   *Antennarius sanguineus*: a, late postflexion, 6.7 mm (CalCOFI 5612, station 163G.30); b, benthic juvenile, 8.6 mm (SIO 62-55).

of dorsal soft rays may be anterior to posterior. Full complements of soft dorsal (12–14), anal (6–8), and caudal (9) fin rays are present by midflexion. Most pectoral and pelvic fin rays also are present by midflexion, and full complements (10–12 and I,5, respectively) are completed during the postflexion stage. Addition of pectoral fin rays is ventrad. The spine is the last element to form in the pelvic fin. All three cephalic spines form during the flexion stage: the third spine forms first, followed by simultaneous development of the first two spines. The illicium (the first cephalic spine) remains unornamented

until settlement, when it acquires a simple escal swelling (fig. 3). The first escal filaments form at ca. 13 mm, and by 20 mm the esca is approaching the typical adult form (fig. 3).

The state of dorsal- and anal-fin pterygiophore development in the preflexion stage could not be determined with certainty owing to the poor staining of the specimen: the cartilaginous pterygiophore of the third cephalic spine is forming; at least the anterior nine or ten dorsal soft-ray pterygiophores are present in cartilage; and no anal-fin pterygiophores are visible (fig. 4a).
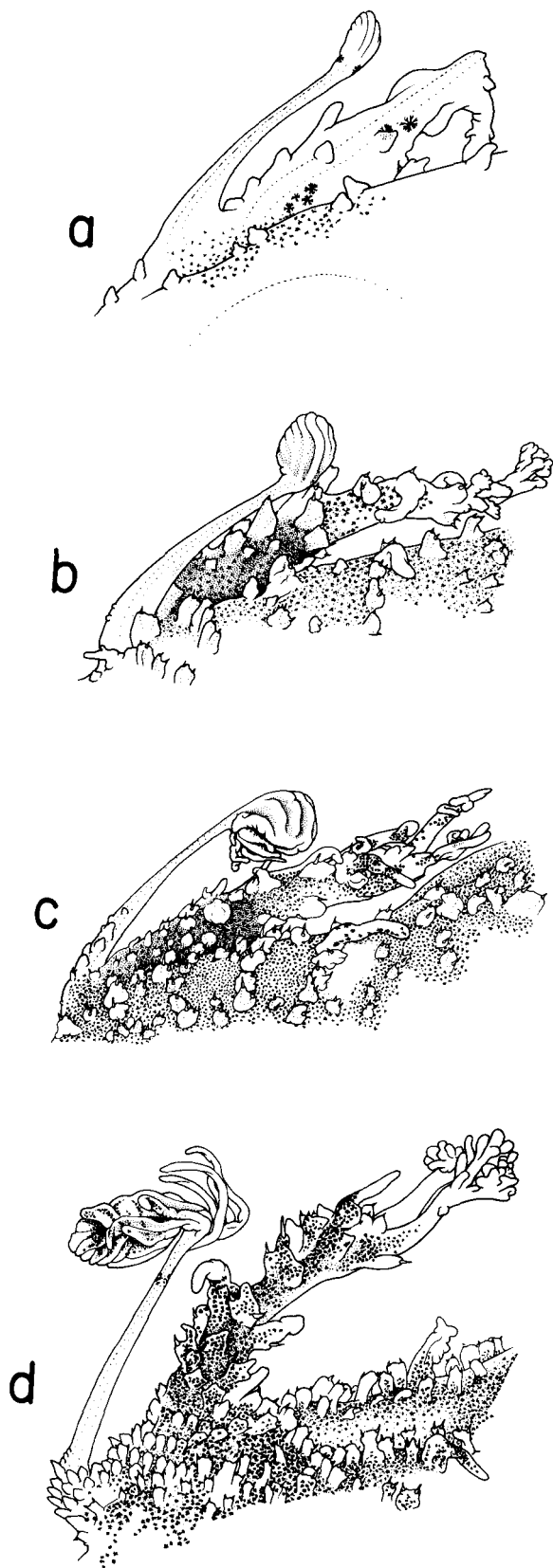
Figure 3. Development of the esca in benthic juveniles of *Antennarius sanguineus*: a, 8.1 mm (SIO 62-55); b, 9.5 mm (SIO 62-55); c, 12.6 mm (SIO 62-55); d, 19.8 mm (SIO 61-242).

All second dorsal- and anal-fin pterygiophores are present in cartilage in the 2.8 mm flexion-stage specimen. Although none of the pterygiophores clearly consists of separate proximal and distal radials at this stage, it appears that distal radials are beginning to detach from the ends of dorsal pterygiophores 4–11 in this specimen (fig. 4b). By early postflexion, dorsal rays 3–11 and anal rays 3–6 are clearly supported by separate cartilaginous distal radials (fig. 5a). The distal radial supporting dorsal ray 2 separates from the first pterygiophore a little later; the first proximal radial supports the first dorsal soft ray. The last pterygiophore, supporting the last dorsal ray, does not divide into proximal and distal radials. Likewise, the first and last anal-fin pterygiophores, supporting the first and last anal rays, do not separate into proximal and distal elements. The second anal ray articulates with the proximal radial of the second anal pterygiophore (fig. 5b). In the soft dorsal fin, pterygiophore ossification begins by early postflexion; each proximal radial may ossify initially at the middle of its anterior margin (as in the last two dorsal pterygiophores of the 3.6 mm specimen, fig. 5a). From this initial site, bone forms around the middle of each radial, then spreads along its length so that by late postflexion only the proximal tip and distal margin remain cartilaginous (fig. 5b). The central proximal radials may be the first to begin ossifying in the soft dorsal fin. Proximal radials of the anal-fin pterygiophores ossify at the same time, and each apparently ossifies in the same way, as the dorsal proximal radials. It is unclear whether the anal-fin pterygiophores ossify simultaneously or sequentially. Distal radials do not ossify during larval development in either fin.

The rodlike, cartilaginous pterygiophore of the third cephalic spine forms in the preflexion stage, and that of the first two spines forms during notochord flexion. All three spines are supported on somewhat compressed dorsal extensions of their pterygiophores. Each pterygiophore begins to ossify around the middle of its elongate shaft during the postflexion stage; the third spine probably begins to ossify first. Simultaneously with (or soon after) initial ossification of the shaft of the illicial pterygiophore, thin crescent-shaped ossifications form around the anterolateral margins of the spine supports below the illicium and second cephalic spine. These subsequently spread up the supports and by late postflexion form a thin flange pierced by a foramen below each spine. A pair of hooklike extensions from the base of each spine fits into its adjacent foramen. A similar flange and foramen supports the third cephalic spine, but it is unclear whether this ossification spreads forward from the pterygiophore shaft or originates independently.

In the preflexion specimen the first 16 neural arches are ossifying: the first six pairs of neurapophyses are ossified along their full length (or nearly so), the next
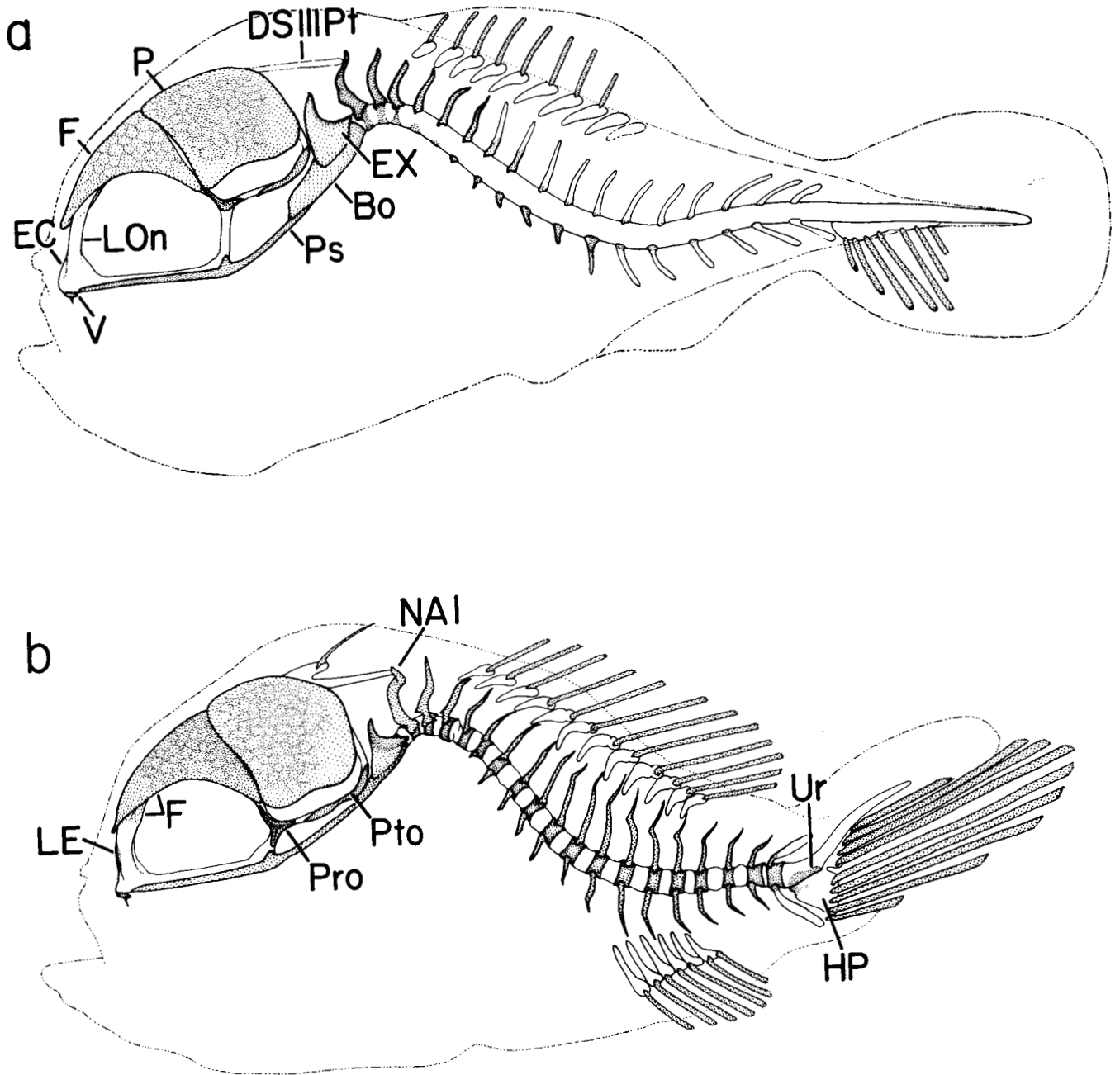
223

Figure 4. Development of the axial skeleton and skull of *Antennarius sanguineus*: *a*, preflexion, 2.9 mm (CalCOFI 5209, station 153G.32); *b*, flexion, 2.8 mm (CalCOFI 5708, station 151G.100). White = cartilage; stippled = ossifying. Abbreviations are Bo, basioccipital; DSIIIPt, pterygiophore of the third cephalic spine; EC, ethmoid cartilage; Ex, exoccipital; F, frontal; HP, hypural plate; LE, lateral ethmoid; LOn, lamina orbitonasalis; NA1, first neural arch; P, parietal; Pro, prootic; Ps, parasphenoid; Pto, pterotic; Ur, urostyle; V, vomer.

two pairs are ossifying on about the lower third, and the remainder are ossifying only at their bases (fig. 4a). The direction of ossification of each arch is thus proximal to distal. The first three neural arches are open distally (arches 2 and 3 are nearly closed) in the preflexion specimen. By late flexion all 3 are closed and all 18 neural arches are ossified, as are the neural spines on arches 2

and 7–17 (fig. 4b). Arches 1 and 3–5 lack neural spines, and the last neural spine is cartilaginous during the flexion stage. As the larvae grow the neural spines on arches 6–9 become spatulate and relatively shorter, barely interdigitating with the dorsal pterygiophores early in the postflexion stage (fig. 5a) and not interdigitating at all by late postflexion (fig. 5b). Neural arches 3–5 also
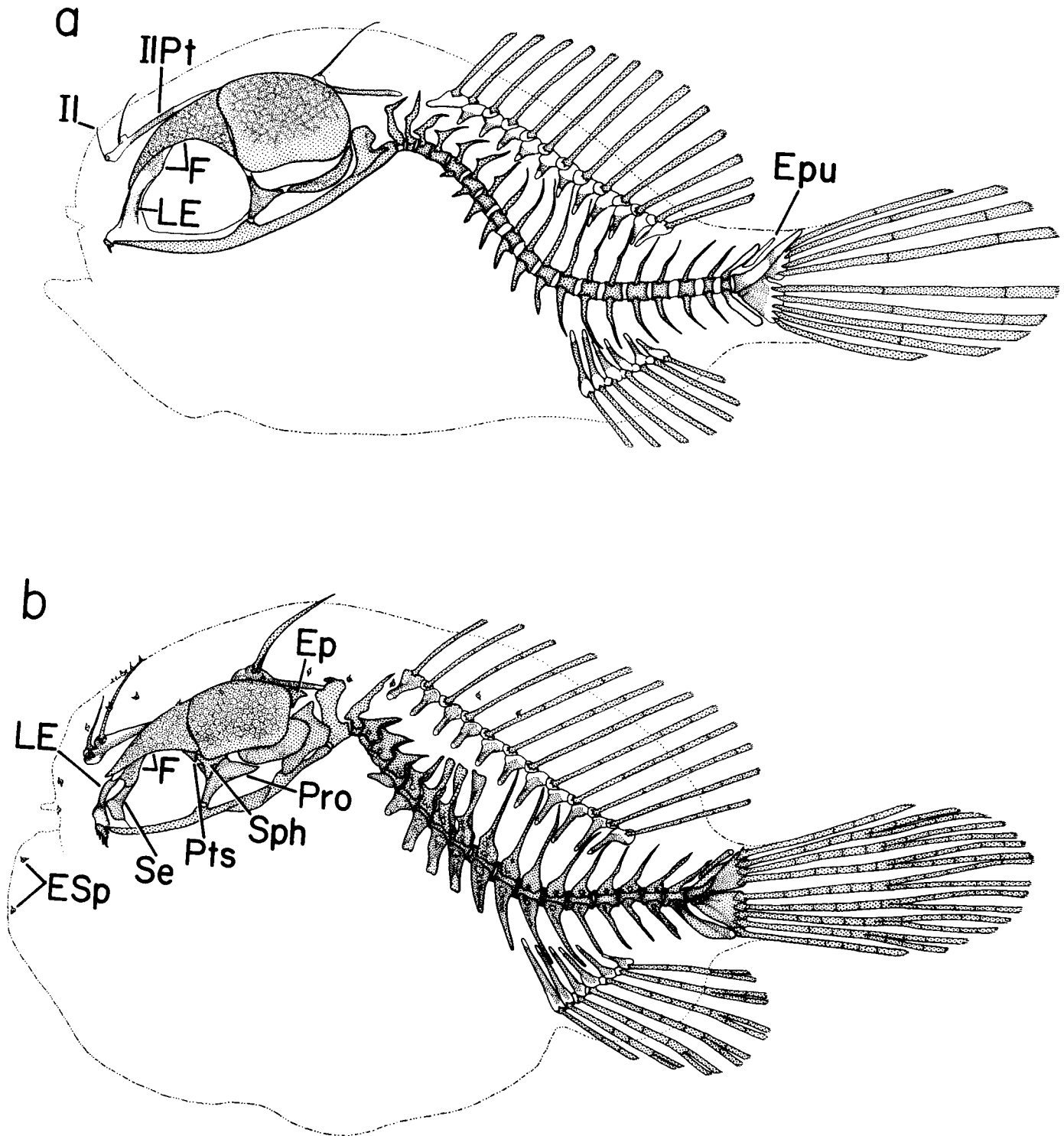
Figure 5.   Development of the axial skeleton and skull of postflexion stage *Antennarius sanguineus*: *a*, 3.6 mm (CalCOFI 5706, station 153.20); *b*, 8.1 mm (TO 58-1, station 105). White = cartilage; stippled = ossifying. Abbreviations are Ep, epiotic; Epu, epural; ESp, epidermal spinule; Il, illicium; IlPt, illicial pterygiophore; Pts, pterosphenoid; Se, supraethmoid; sph, sphenotic. For other abbreviations see figure 4.

no longer interdigitate with the dorsal pterygiophores after early postflexion.

At least 12 pairs of haemapophyses and haemal arches are present in the preflexion specimen: the anterior five pairs of small haemapophyses appear to be mostly ossified, the sixth (at the site of the future first caudal vertebra) is ossifying on about its proximal third, the seventh through tenth at their bases only, and the last two are cartilaginous (fig. 4a). The direction of ossification of each haemal arch is thus distad from the base. By late flexion all haemal arches and spines are ossifying, except the posteriormost spine, which ossifies during the postflexion stage. This last haemal spine becomes broad and compressed by late postflexion and may partially support the lowermost caudal fin ray (fig. 5b).

It could not be determined with certainty whether any vertebral centra were ossifying in the preflexion specimen, but it appears that the first three abdominal centra might be present as thin rings around the notochord below the first three neural arches, and the fourth forming as a ventral ossification on the notochord opposite the fourth neural arch (fig. 4a). It is unclear whether a small ventral ossification corresponding to the fifth abdominal vertebra is the vertebra beginning to form, or the haemapophyses beginning to ossify, or both. In the 2.8 mm flexion-stage specimen, all the vertebrae are forming: the first 18 are present as ossifying rings around the notochord, and the urostyle is represented by a ventral ossification on the notochord adjacent to the anterior (= lower) section of the hypural plate (fig. 4b). The 3.6 mm postflexion specimen apparently has a second urostylar ossification site adjacent to the upper section of the hypural plate (fig. 5a), suggesting that the urostyle ossifies from both ends toward the middle (perhaps corresponding to ossification from an ancestral preural centrum 1 + ural centrum 1 proximally and ural centrum 2 distally?). There are 10–11 (nearly always 10) abdominal vertebrae and 9 caudal vertebrae, including the urostyle.

The hypural plate is a slender, triangular cartilage posteriorly below the notochord in the preflexion specimen, and has become a deeply notched, ossifying plate supporting all 9 caudal rays in the 2.8 mm flexion-stage specimen (fig. 4). Hypural ossification begins during notochord flexion, along the proximal margin of the anterior (= lower) section, and spreads both distad and along the hypural base onto the upper section by postflexion. The single epural cartilage forms early in the postflexion stage and ossifies except at its distal tip by late postflexion. A single pair of uroneurals ossifies along the dorsal margin of the urostyle and upper hypural plate in the postflexion stage (fig. 5b).

The pectoral girdle of the preflexion specimen consists of slender, ossified cleithra, postcleithra (only the

ventral postcleithra form), and supracleithra (fig. 6a). A small coracoscapular cartilage is present. Owing to the poor staining of the specimen, it could not be determined whether the pectoral-fin base consists of a single cartilage pierced by a large foramen, or two cartilages, the lower larger than the upper. By late flexion the post-temporals have begun ossifying at the upper ends of the supracleithra; there definitely are separate upper and lower pectoral cartilages; and a foramen is present in the middle of the lower, larger cartilage. Ossification of the pectoral radials begins early in the postflexion stage around the middle of the upper cartilage and the middles of the two lower radials that are being defined by the elongating foramen in the lower cartilage (fig. 6b). By late postflexion the upper radial is completely ossified except at its tips, and the lower radials, which remain fused at both ends, are cartilaginous only at their proximal tip and in a band along their distal margin. Small, cartilaginous distal pectoral radials form along the margin of the lower proximal radials late in the postflexion stage; these support the pectoral fin rays (fig. 6c).

The elongate cartilaginous coracoid process regresses after the early part of the postflexion stage, and the scapula and coracoid ossify on the upper and lower half, respectively, of the coracoscapular cartilage late in the postflexion stage (fig. 6c). Cartilaginous basipterygia form during notochord flexion and ossify, beginning around the middle and spreading toward both ends, during the postflexion stage (fig. 6b). By late postflexion each basipterygium is ossified except at its proximal tip and distal margin (fig. 6c).

The neurocranium is already becoming well ossified in the 2.9 mm preflexion specimen (fig. 4a). Ossifying bones include the frontals, parietals, supraoccipital, prootics, pterotics, exoccipitals, basisphenoid, parasphenoid, and vomer. The frontals initially closely approach one another mesially, except for a small anterior mesial notch and groove, which subsequently widens and deepens. During the postflexion stage the supraethmoid ossifies on the ethmoid cartilage below this widening gap (fig. 5b). The groove receives the posterior section of the illicial pterygiophore. The parietals initially nearly touch one another mesially; the small, oval supraoccipital is located mesially at their posterior margins but barely separates them. However, as the supraoccipital grows anteriorly between the parietals during the postflexion stage, they become increasingly widely separated. Epiotics ossify behind the parietals during the postflexion stage, and together with the exoccipitals form most of the posterior part of the brain case. A shallow groove between the parietals (the supraoccipital is its floor) and extending between the epiotics receives the anterior part of the third cephalic spine pterygiophore. The prootic initially is a thin, V-shaped ossification on the cartilage forming
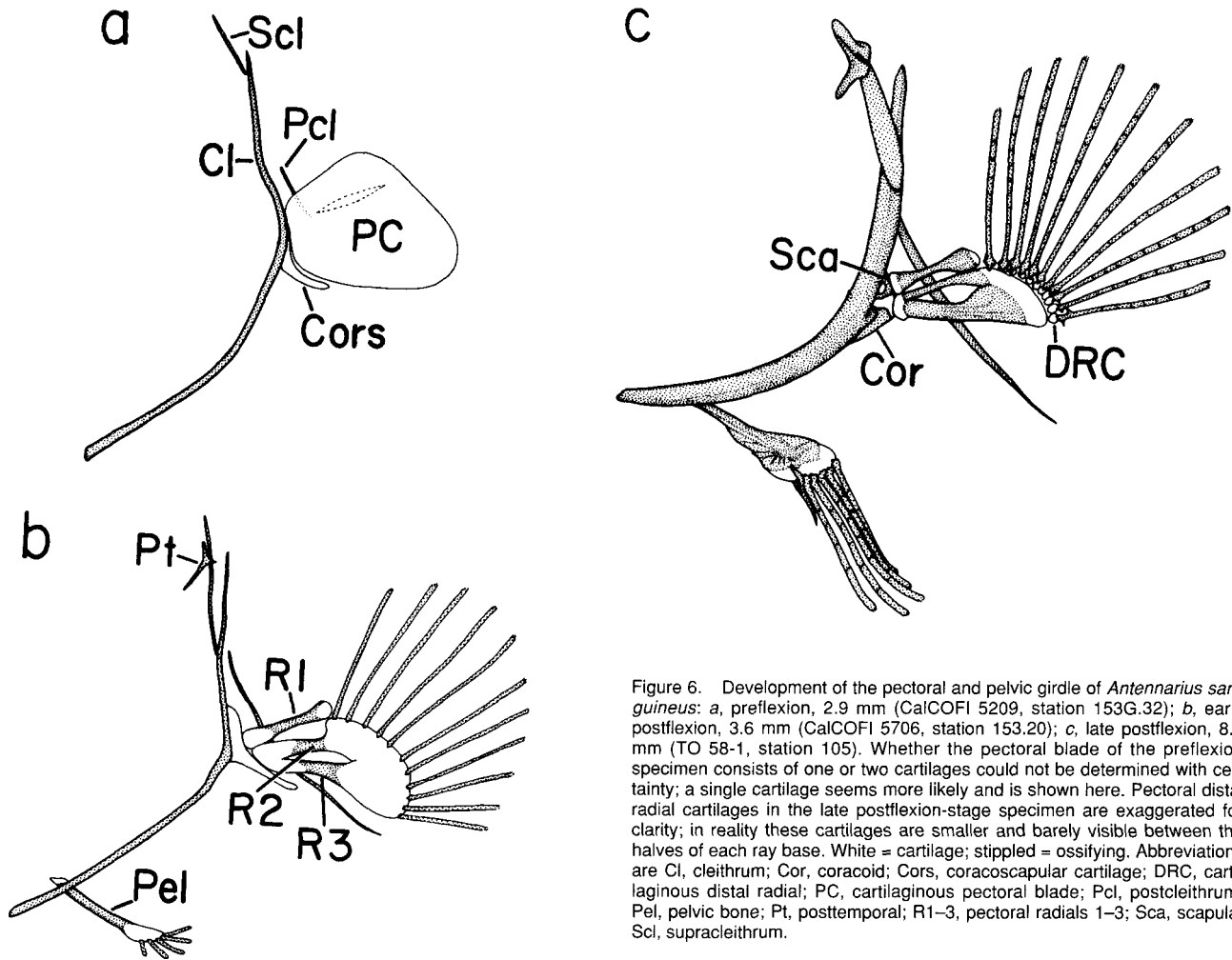
Figure 6.   Development of the pectoral and pelvic girdle of *Antennarius sanguineus*: a, preflexion, 2.9 mm (CalCOFI 5209, station 153G.32); b, early postflexion, 3.6 mm (CalCOFI 5706, station 153.20); c, late postflexion, 8.1 mm (TO 58-1, station 105). Whether the pectoral blade of the preflexion specimen consists of one or two cartilages could not be determined with certainty; a single cartilage seems more likely and is shown here. Pectoral distal radial cartilages in the late postflexion-stage specimen are exaggerated for clarity; in reality these cartilages are smaller and barely visible between the halves of each ray base. White = cartilage; stippled = ossifying. Abbreviations are Cl, cleithrum; Cor, coracoid; Cors, coracoscapular cartilage; DRC, cartilaginous distal radial; PC, cartilaginous pectoral blade; Pcl, postcleithrum; Pel, pelvic bone; Pt, posttemporal; R1–3, pectoral radials 1–3; Sca, scapula; Scl, supracleithrum.

the anteroventral corner of the auditory capsule, while the pterotic is a thin, elongate oval ossification on much of the lower part of the capsule (fig. 4a). The prootic becomes Y-shaped during the flexion stage, with its lower arm extending mesially and ventrad toward the ascending arm of the parasphenoid (fig. 4b). During the postflexion stage the upper sections of the prootics expand to form much of the anteroventral part of the brain case. The foramen of the trigeminofascialis nerve complex is visible in each prootic, adjacent to the lower end of the sphenoid. The pterotics expand during postflexion to become large, roughly oval bones forming much of the ventrolateral part of the brain case. Each has an articular surface on its lower center that articulates with the pterotic process of the adjacent hyomandibula. During the postflexion stage the sphenotics ossify below the anteroventral corners of the parietals and lateral to the anterodorsal ends of the adjacent prootics (fig. 5b). Each roughly T-shaped sphenotic bone articulates with the sphenotic process of the adjacent hyomandibula. A small, triangular pterosphenotic bone ossifies between the pos-

teroventral edge of each frontal and the adjacent prootic during the postflexion stage (fig. 5b).

The vomer is a small, crescent-shaped bone bearing a small tooth at each end, located ventrally on the ethmoid cartilage at the anterior end of the parasphenoid in the preflexion specimen (fig. 4a). The vomer lengthens and broadens with larval growth, and teeth are added sequentially toward the middle during postflexion. Thin, oval, lateral ethmoids begin to ossify on the slender lamina orbitonasalis cartilages during the flexion stage (fig. 4b). Ossification spreads along and around each cartilage during the postflexion stage, resulting in somewhat compressed, cylindrical lateral ethmoids that flare ventrally by late postflexion (fig. 5b).

The premaxillae, maxillae, dentaries (with four teeth), and articulars are ossifying in the 2.9 mm preflexion specimen, but the degree of development of these bones could not be determined with any certainty owing to the poor staining of the specimen. The premaxillae of the flexion-stage and early postflexion-stage specimens are slender bones, each of which tapers to a point distally,

bears two or three small teeth proximally, and has a small, rounded, articular process posteriorly and a long, slender, ascending process dorsally at its proximal end (fig. 7a, b). The ascending processes gradually lengthen, extending into the groove anteriorly between the frontals. At the same time the articular processes greatly enlarge, and— during the latter part of the postflexion stage—a long, slender postmaxillary process extends posteromedially from the proximal end of each premaxilla (fig. 7c). The number of premaxillary teeth increases to 13 or 14 on each (all small, especially distally). Maxillae in the younger specimens are flat and moderately wide distally but taper and become quite slender along the proximal third, except that the proximal end is flared into a broad V shape, with the anterolaterally projecting wing overlapping the base of the premaxillary ascending process, and the anteromedially projecting wing nearly reaching the premaxillary articular process (fig. 7). The maxillae change little during subsequent larval development, except to become broader.

The dentaries are slender, Y-shaped bones (fig. 7) that abut at their proximal ends and bear a single row of a few teeth in the flexion-stage and early postflexion-stage specimens. During the postflexion stage the dentaries broaden, and the upper arm of the "Y" becomes longer than the lower. By late postflexion the number of teeth has increased to about 20 in the outer row on each dentary, and an inner row of smaller teeth is forming. The articular is a broad, T-shaped cartilage with its base extending forward between the arms of the dentary "Y," and ossifying on its base and lower arm in the flexion and early postflexion specimens (fig. 7). A notch on the posterior margin of the lower arm ossifies early and articulates with the quadrate (fig. 7a). The articular subsequently changes little in shape except to become broader and to acquire a posteroventral flange by late postflexion (fig. 7c). The angular is ossifying on the posteroventral margin of the articular cartilage in the flexion specimen, and by late postflexion it has become a roughly triangular bone that fits into a notch in the lower posterior articular margin (fig. 7).

The degree of development of the elements of the suspensorium is unclear in the preflexion specimen. Thin ossifications distally on the anterior and ventral arms of the palato-pterygoquadrate cartilages represent the palatines and quadrates, respectively, and the hyomandibulae are ossifying at least on their sphenotic, pterotic, and opercular processes, but whether any other bones of the suspensorium are ossifying cannot be determined. By the flexion stage the quadrate has ossified on the entire lower arm of each palato-pterygoquadrate cartilage; the palatine occupies about the anterior half of the anterior arm of each cartilage; the slender mesopterygoid is ossifying between the palatine and
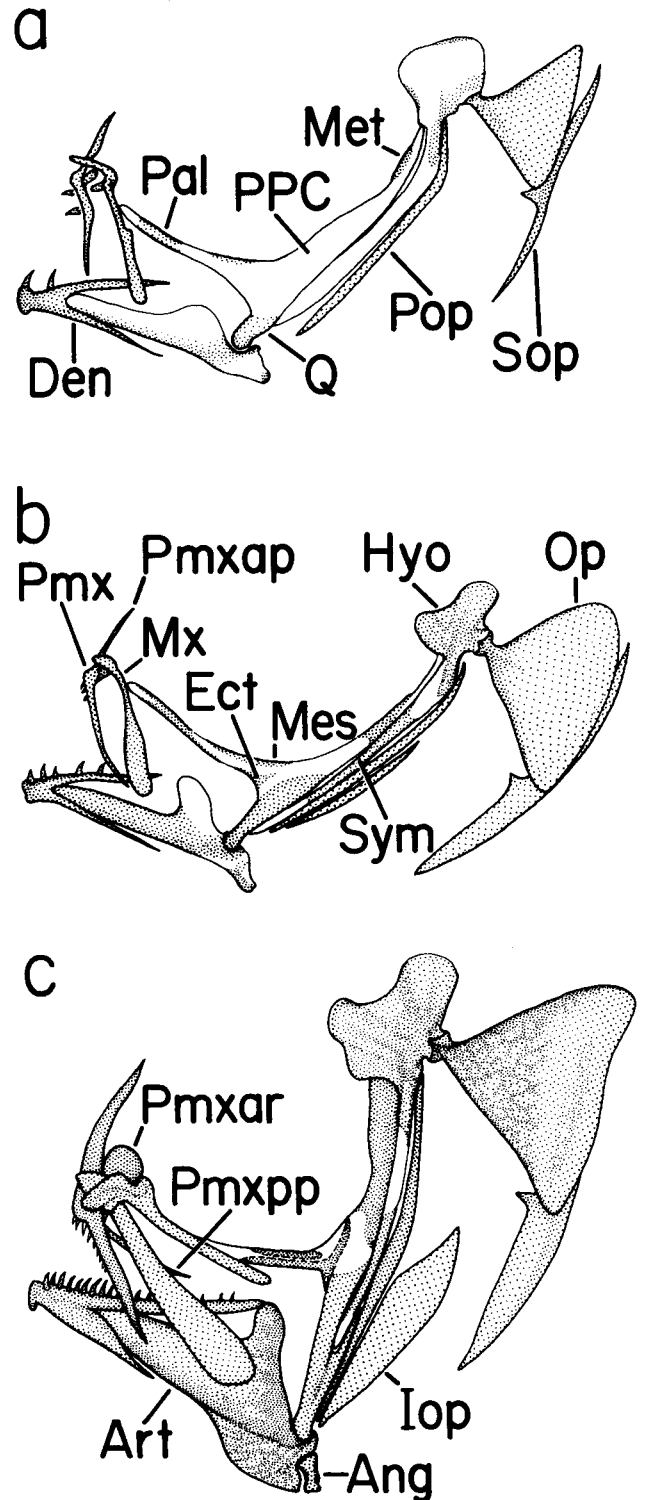

Figure 7. Development of the jaws, suspensorium, and opercular bones of *Antennarius sanguineus*: *a*, flexion, 2.8 mm (CalCOFI 5708, station 151G.100); *b*, early postflexion, 3.6 mm (CalCOFI 5706, station 153.20); *c*, late postflexion, 8.1 mm (TO 58-1, station 105). White = cartilage; stippled = ossifying. Abbreviations are Ang, angular; Art, articular; Den, dentary; Ect, ectopterygoid; Hyo, hyomandibula; Iop, interopercle; Mes, mesethmoid; Met, metethmoid; Mx, maxilla; Op, opercle; Pal, palatine; Pmx, premaxilla; Pmxap, ascending process of the premaxilla; Pmxar, articular process of the premaxilla; Pmxpp, postmaxillary process of the premaxilla; Pop, preopercle; PPC, palato-pterygoquadrate cartilage; Q, quadrate; Sop, subopercle; Sym, symplectic.

quadrate on the dorsal margin of the cartilage; and the metapterygoid is a small, slender distal ossification on the anterior margin of the upper arm of the cartilage (fig. 7a). During the postflexion stage the palatine develops a flattened anterolateral process that overlaps the upper end of the maxilla, and a flattened anteromedial process that lies adjacent to the lateral ethmoid. Palatine teeth form on the mesial surface along the middle of each palatine beginning late in larval development. The T-shaped ectopterygoid ossifies ventrally on the anterior arm of the palato-pterygoquadrate cartilage between the palatine and quadrate and below the mesopterygoid during the postflexion stage (fig. 7b, c). The symplectic ossifies on the lower part on the hyomandibulosymplectic cartilage during the postflexion stage.

Among the opercular series bones, only the opercles are clearly ossifying, at least in the vicinity of their articulations with the hyomandibulae, in the preflexion specimen, but whether any other opercular series bones are forming could not be determined. A broad, triangular opercle, together with the slender subopercle and the elongate, very slender preopercle are present on each side in the flexion-stage specimen, and the slender interopercle is added early in the postflexion stage (fig. 7). The proximal end of the opercle is more or less flattened where it meets the hyomandibula in the flexion stage, but by early postflexion this articular surface of the opercle has become a shallow cup which attaches in a ball-and-socket joint to the cartilaginous end of the opercular condyle of the hyomandibula (fig. 7). The subopercle elongates somewhat during the postflexion stage as its lower part simultaneously broadens. The interopercle likewise elongates a bit and broadens during postflexion. The preopercle is also a very long bone, but it remains quite slender.

Each hyoid arch of the preflexion specimen is largely cartilaginous, with thin ceratohyal, epihyal, and interhyal ossifications anteriorly and posteriorly around the cartilage (fig. 8a). It appears that there are small, thin, oval dorsal and ventral hypohyal ossifications at the anterior end of the hypohyal cartilage, as well. All six branchiostegal rays are ossified: the anterior two articulate with the ceratohyal, and the posterior four are supported by the broad hyoid cartilage. The ceratohyal ossification spreads posteriorly onto this broad section of the cartilage by early postflexion, so that all six branchiostegal rays are supported by the ceratohyal. The middle two branchiostegal rays curve downward distally to support the gill opening below the pectoral fin base. A small, triradiate urohyal bone forms early in the postflexion stage. One arm of the urohyal is directed dorsally and the other two are directed posteriorly, so that the urohyal appears to be more or less V-shaped in lateral and ventral views. A small, posteriorly directed, median urohyal flange be-
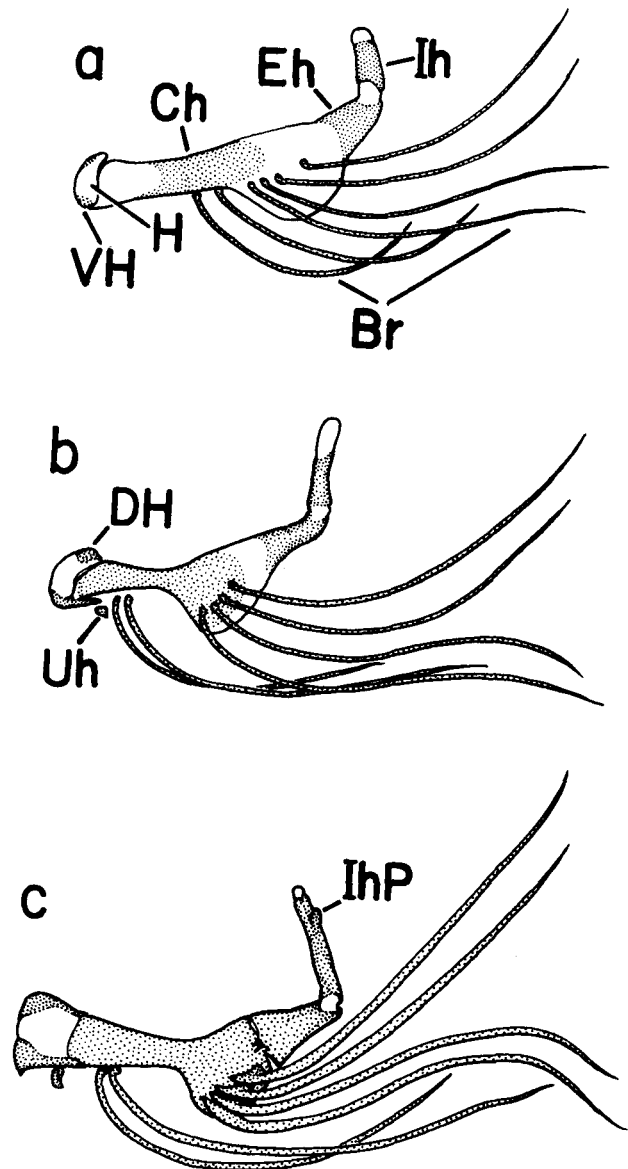

Figure 8. Development of the hyoid arch of *Antennarius sanguineus*: a, preflexion, 2.9 mm (CalCOFI 5209, station 153G.32); b, early postflexion, 3.6 mm (CalCOFI 5706, station 153.20); c, late postflexion, 8.1 mm (TO 58-1, station 105). White = cartilage; stippled = ossifying. Abbreviations are Br, branchiostegal rays; Ch, ceratohyal; DH, dorsal hypohyal; Eh, epihyal; H, hypohyal cartilage; Ih, interhyal; IhP, dorsolateral process of the interhyal; Uh, urohyal; VH, ventral hypohyal.

gins to form during the latter part of the postflexion stage. The interhyal remains a simple cylindrical bone until late postflexion, when a short posterodorsal process forms on its upper lateral surface (fig. 8c). The posterior margin of the preopercle rides on the anterior face of this interhyal process.

The basibranchial(s), gill arches, and second pharyngobranchial tooth plates (each with three teeth) are visible in the preflexion specimen, but apart from the tooth plates and ceratobranchials 1 and 2 ossifying on the middles of their respective arches, it could not be determined

whether any other bones of the branchial arches were forming. In the flexion-stage specimen all three pharyngobranchials, four epibranchials, five ceratobranchials, and at least hypobranchials 1 and 2 and basibranchials 1 and 2 are ossifying. All are simple, flattened to cylindrical, rodlike bones. The second pharyngobranchials still bear three teeth each, and each of the fifth ceratobranchials has acquired a single dorsal tooth anteriorly. The number of teeth increases to four and two, respectively, by early postflexion; by late postflexion there are many teeth on the second pharyngobranchials and fifth ceratobranchials. Beginning early in the postflexion stage the second and third hypobranchials broaden proximally, and by late postflexion both have become Y-shaped. Late in the postflexion stage, epibranchial 1 begins to broaden distally; presumably it is beginning to acquire the triradiate adult shape described by Pietsch (1981).

Pigmentation. The inflated skin is unpigmented throughout the larval phase of development. "External" pigmentation described below refers to subdermal melanophores on the surface of the musculature; "internal" pigmentation refers to melanophores that are more deeply internal. The principal elements of the larval pigment pattern are melanophores dorsally on the head and nape; dorsally and laterally on the gut; internally, anteroventrally in the tail; and both internally and externally in a bar posteriorly on the tail. The preflexion specimen has melanophores on the posterior margin of the midbrain and dorsally on the hindbrain, a dense shield of melanophores over the upper 60%–70% of the gut, a large internal melanophore anteriorly on each side of the gut mesial to the cleithra at the level of the pectoral-fin origin, and a bar posteriorly on the tail (at ca. myomeres 14–16) consisting primarily of external, myoseptal melanophores (fig. 1a).

Pigmentation on the head subsequently increases: more melanophores are added on the mid- and hindbrain, and midway through the postflexion stage a few melanophores begin to form on the opercular area, increasing in number and spreading anteroventrally to below mid-eye by late postflexion, but still remaining somewhat sparse. Internal melanophores form in the nape area by the beginning of notochord flexion; these are primarily myoseptal, commonly continuous with the hindbrain pigment, and extend posteriorly to about the third myomere by the postflexion stage. During postflexion this pigment may extend ventrad to the level of the gut, or it may remain predominantly dorsal. External myoseptal melanophores form in the same area during the postflexion stage, spreading posteriorly sometimes as far as midtail by the end of the larval phase. This external pigmentation is light to moderate.

Gut pigmentation changes little during larval development: the shield covers a variable proportion of the gut (approximately the upper 25%–75%), and the terminal section of the hindgut always is unpigmented. Ventral gut pigment is also lacking, both in larvae and in benthic juveniles smaller than ca. 20 mm.

Internal melanophores form along the haemal arches beginning at about the last preanal myomere at the beginning of flexion, and slowly proliferate caudad below the vertebral column to about midtail by halfway through the postflexion stage. The tail bar gradually broadens, extending from myomeres 12–14 through 16–17 by the postflexion stage. External and internal pigmentation in the bar increase: external melanophores are predominantly myoseptal and on the horizontal septum, whereas internal melanophores are primarily above and below the vertebral column. The bar may extend onto the bases of the adjacent dorsal and anal fin rays by late flexion, and the external pigment usually extends forward ventrolaterally during the postflexion stage. In two of the larger postflexion-stage specimens, myoseptal melanophores are sparsely scattered along nearly the full length of the tail.

All of the larval pigmentation becomes increasingly obscure as the skin thickens and becomes opaque during the latter part of the postflexion stage, and it apparently decreases at settlement: the only such pigment consistently visible through the skin of recently settled individuals is on the horizontal septum of the tail and on the gut. Dissection reveals some additional small melanophores scattered dorsolaterally on the head, trunk, and tail.

Juvenile pigmentation first begins to appear as minute melanophores on the epidermis, initially mainly on the head and trunk, soon after settlement. These begin to resolve into the typical spotted adult pattern by ca. 20 mm. The spots are first discernable dorsally on the trunk and tail, and cover the body by ca. 30 mm.

The esca is lightly pigmented ventrally when it forms at settlement (fig. 3). A more or less even to irregularly striped pattern develops on the main body of the esca after the escal filaments begin to form. The first stripe forms on the illicium just below the esca at ca. 20 mm, and stripes are added toward the base of the illicium. The second cephalic spine begins to become pigmented at settlement.

Shortly after settlement (ca. 8.5 mm) melanophores form proximally on the first and last pelvic and pectoral fin rays (fig. 2b). By ca. 10 mm, bands are added distally on the pectoral, pelvic, and caudal fins, and the proximal pectoral and pelvic spots expand to small blotches. Another band is added on the pectoral and pelvic fins, and another one or two bands are added on the caudal fin by 13 mm. A large blotch forms proximally on the posterior part of the dorsal fin (ca. D10) by 13 mm, and additional smaller blotches form along

the bases of some of the anterior dorsal fin rays and at the base of the last anal fin ray by ca. 16 mm. By ca. 20 mm several small blotches are scattered on the dorsal fin, and a distal stripe is present on the anal fin.

Antennatus strigatus (Gill 1863) Bandtail Frogfish

Morphology. Larvae generally resemble those of *Antennarius sanguineus* but are slightly more elongate, with a slightly larger head and smaller eye (table 2; figs. 9 and 10). The most striking morphological differences between the two species are the small larval size and the early development of dermal spinules in *Antennatus.* The smallest specimen of *A. strigatus,* 2.3 mm, already has completed notochord flexion, full complements of rays in all fins except the pelvic (4 rays forming), a fully formed illicium with slight escal thickening, and widely scattered, predominantly bifurcate, dermal spinules on the body (fig. 9a). Each spinule arises from a low, rounded, fleshy base. As the larvae grow, the number of spinules increases; the area covered by the spinules expands onto the skin covering the proximal parts of the dorsal and anal fins; and the individual spinules become smaller relative to body size (fig. 9b). By ca. 5 mm the lower part of each spinule is enclosed in a small, fleshy papilla (fig. 10a). In juveniles each papilla encloses most of its spinule; only the spinule tips are always exposed.

Pigmentation. Larval pigmentation is unlike that of *Antennarius sanguineus.* Principal elements of the *Antennatus strigatus* pattern are melanophores on the jaws, laterally and ventrally on the cranium, on the opercular area and below the eye, dorsally and dorsolaterally on the gut, and internally around the vertebral column and neural and haemal arches of the trunk and much of the tail (figs. 9 and 10).

In the smallest specimen the dentaries are nearly completely pigmented; a few melanophores are located on the posterior margin and ventrally on the posterior half of the midbrain; the upper ca. 60% of the gut is lightly pigmented; a large melanophore appears anteriorly on each side of the gut mesial to the cleithrum just below the level of the pectoral-fin origin; and the internal trunk and tail pigment extends from the next to last preanal myomere to the third postanal myomere (fig. 9a). Unlike the other three larvae, the 2.3 mm specimen has an external melanophore on each side over the proximal end of the urostyle.

The dentary pigmentation increases, spreading onto the lip and extending ventrad onto the anterior gular area by 3.4 mm. By this size the upper jaw also is pigmented, and the midbrain pigment has spread forward under the forebrain and dorsally onto the lower sides of the fore- and midbrain. The roof of the mouth and ethmoid cartilage are heavily pigmented as well, and a

TABLE 2
Summary of Measurements of *Antennarius strigatus,* Expressed as Percentage of Body Length (BL) or Head Length (HL); for Each Measurement the Range Is Given Above and the Mean Is Given Below

	Planktonic postflexion stage	Benthic juvenile stage
Number of specimens	4	6
Size range (mm)	2.3–5.1	10.6–14.2
Proportions[a]		
Sn-A/BL	64–75	71–84
	72	76
BDi/BL	52–57	
	54	
BD/BL	65–68	53–72
	66	61
HL/BL	44–48	37–44
	46	41
P1L/BL	14–26	24–27
	20	25
P2L/BL	2–18	16–19
	10	17
HW/HL	87–104	100–120
	96	112
SnL/HL	14–20	15–20
	16	18
ED/HL	29–37	21–26
	33	24

[a]Measurements include preanal length (Sn-A), body depth inclusive (BD) and exclusive (BDi) of the inflated skin, head length (HL), pectoral fin length (P1L), pelvic fin length (P2L), head width (HW), snout length (SnL) and eye diameter (ED).

few melanophores have formed on the opercular area, extending to below mid-eye (fig. 9b). All of this pigment increases so that by 5.1 mm the head is nearly completely pigmented except on the dorsum (fig. 10a). Pigmentation on the gut becomes denser, but otherwise changes little. The internal trunk and tail pigment first spreads forward to nearly the full length of the trunk by 3.4 mm, then spreads dorsally to near the dorsal margin by 5.1 mm. The fins are unpigmented except that a few small melanophores form in the pectoral axil by 5.1 mm.

None of the larval pigmentation is visible externally, and dissection reveals that none remains in small benthic juveniles (11–12 mm). The opaque skin is lightly mottled and densely covered with unpigmented papillae; a pattern of irregular, large, light spots on a darker background begins to emerge by ca. 12 mm. The characteristic striped pattern is present on the fins by 11.6 mm (fig. 10b).

IDENTIFICATION OF LARVAE

Larvae of the three frogfish species that occur in the vicinity of the CalCOFI study area are generally similar in body form and proportions (tables 1 and 2; Watson 1996) and have similar numbers of myomeres (18–20) and fin rays (table 3). However, modal numbers of fin rays distinguish the species (table 3; Pietsch and Grobecker
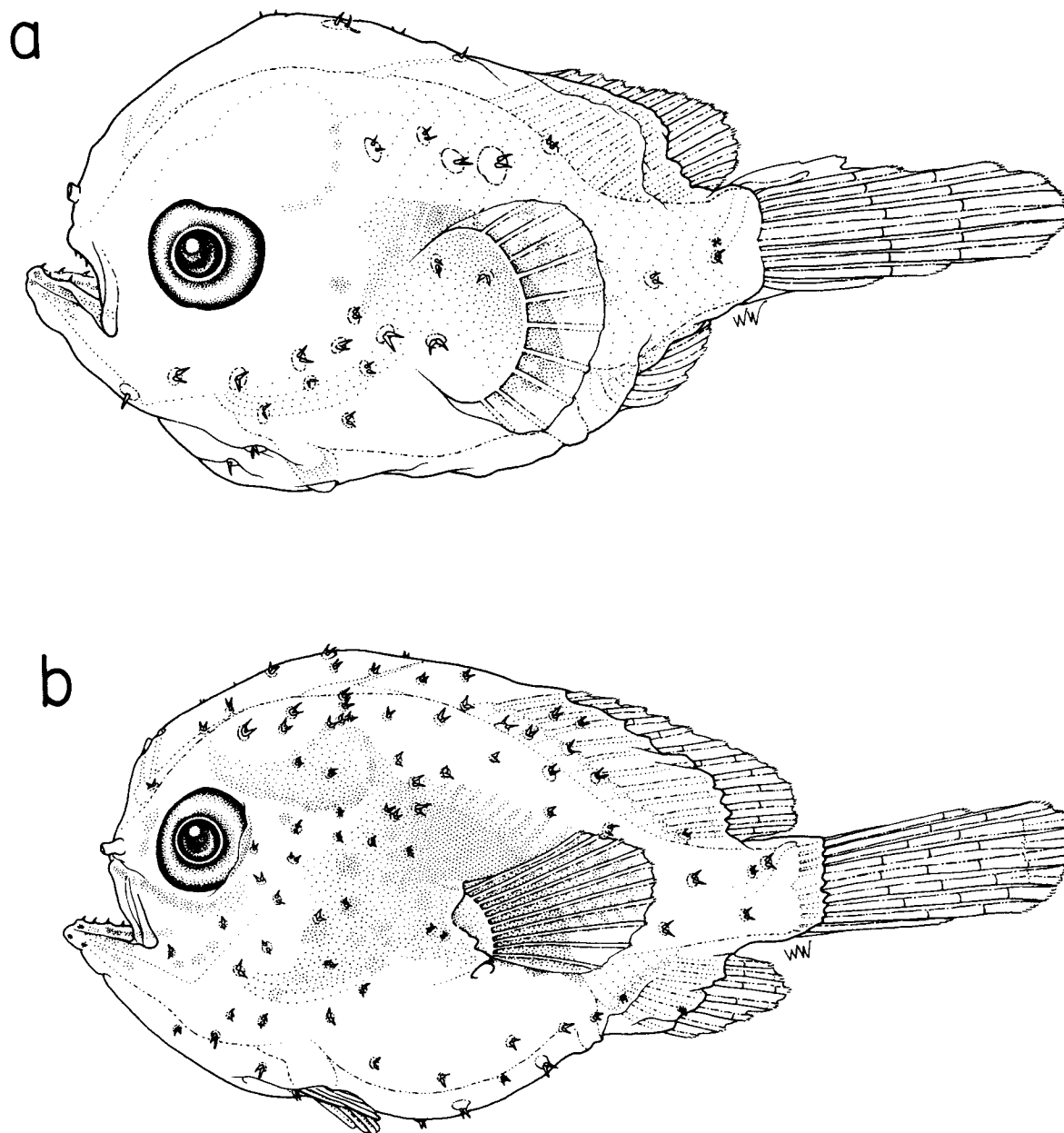
Figure 9. *Antennatus strigatus: a*, 2.3 mm (CalCOFI 5708, station 151G.100); *b*, 3.4 mm (CalCOFI 5708, station 145G.30).

1987), and all three differ in larval pigmentation (figs. 1, 2, 9, 10, 11; Watson 1996). Diagnostic elements of the pigmentation patterns include (1) the internal dorsal melanophore series extending from the nape (early pre-flexion) to mid-tail (by postflexion stage; Watson 1996) and the epidermal melanophores scattered over the head and gut (postflexion stage >ca. 5 mm: fig. 11a) in *Antennarius avalonis*; (2) the mid-tail bar of internal and external melanophores in *A. sanguineus* (all larval stages: figs. 1 and 2); and (3) the jaw pigment and internal melanophores above and below the vertebral column in *Antennatus strigatus* (figs. 9 and 10).

TABLE 3
Selected Fin-Ray Counts for the Antennariid Species of California and Baja California

Species	Dorsal rays	Anal rays	Pectoral rays
Antennarius avalonis	12–14	7–10	11–14
	13	8	13
Antennarius sanguineus	12–14	6–8	10–12
	13	7	11
Antennatus strigatus	11–13	6–8	9–11
	12	7	10

Segmented rays only. Ranges are given above, and modes are given below. Data are primarily from Pietsch and Grobecker 1987, supplemented with counts made during this study.
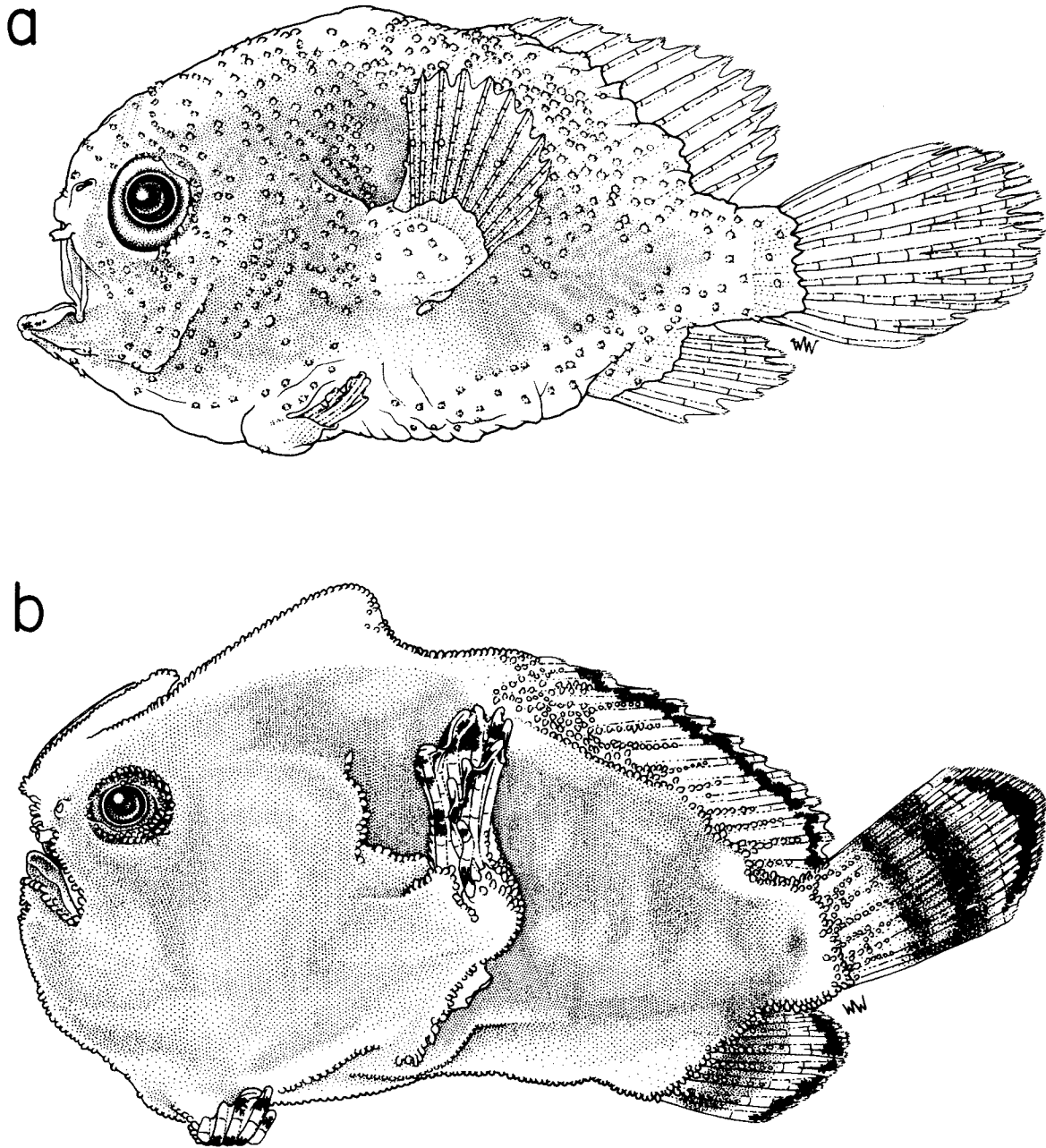
Figure 10. *Antennatus strigatus*: a, postflexion, 5.1 mm (IATTC 90048, station T-3); b, benthic juvenile, 11.6 mm (SIO 67-39). The benthic juvenile is densely covered with small, spinous papillae, but only those around the margins and on the fins are shown.

A. strigatus completes notochord flexion and fin-ray formation at a remarkably small size (<2.3 mm for all but the pelvic fin, which is nearly complete by 2.3 mm); the two *Antennarius* species have begun neither fin-ray development (at least *A. avalonis*, probably both species) nor notochord flexion at this size. *Antennatus strigatus* also begins developing the dermal spinules at a much smaller size than the two *Antennarius* species. The first spinules form by, or before, completion of notochord

flexion in *Antennatus strigatus* but not until late in the postflexion stage in *Antennarius* (ca. 7 mm in *A. avalonis* and 8 mm in *A. sanguineus*). In both *Antennarius* species the spinules initially are completely enclosed (or nearly so) in small, fleshy papillae and become partially exposed after settlement, whereas in *Antennatus* the spinules initially are nearly fully exposed and gradually become enclosed in papillae, finally becoming mostly enclosed after settlement. *A. strigatus* may settle from the
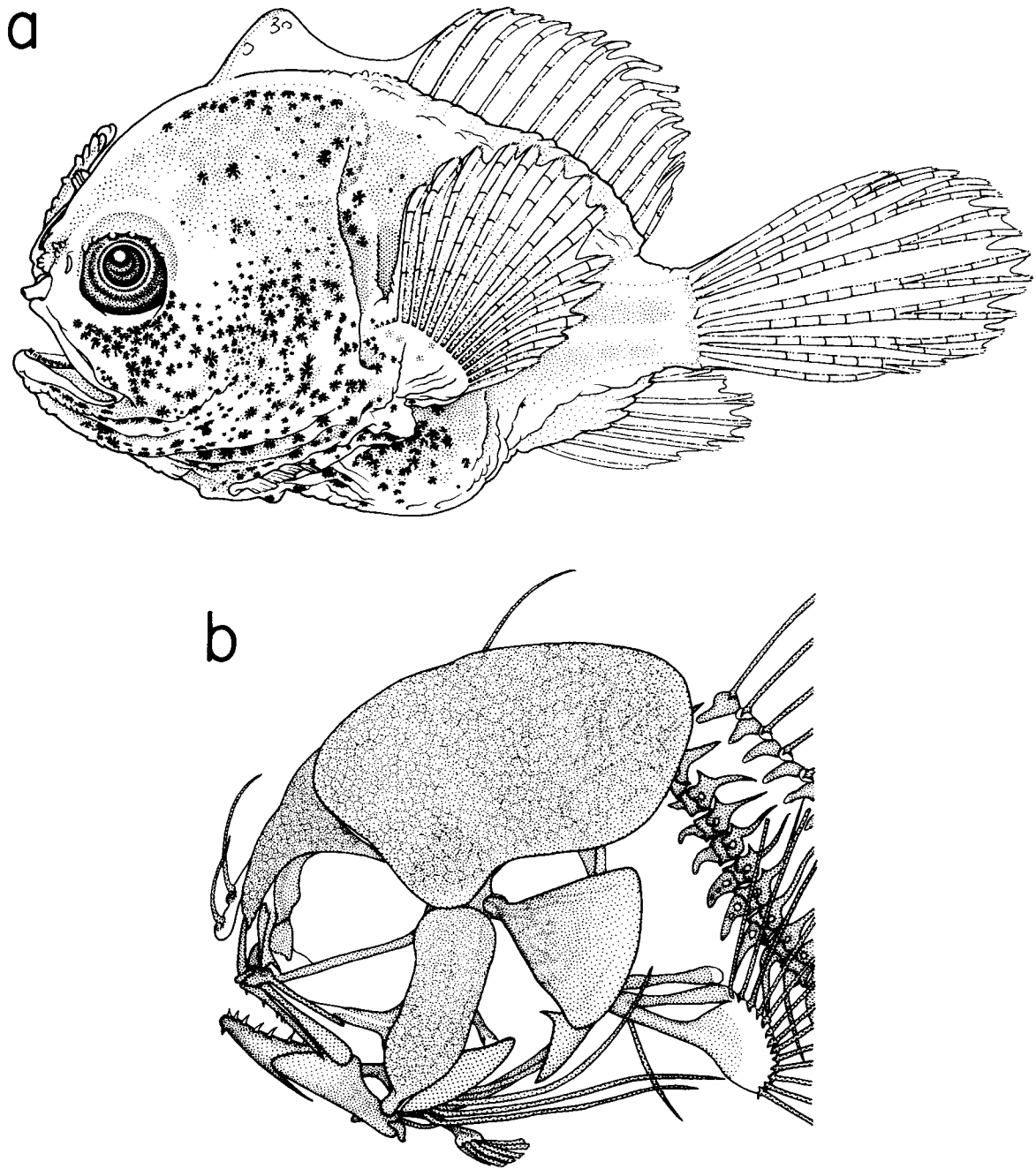
233

Figure 11. *Antennarius avalonis*: *a*, scutatus stage, 7.3 mm (IATTC 91005, station T-8); *b*, skull, pectoral-pelvic girdle, and anterior part of axial skeleton of scutatus stage, 5.3 mm (CalCOFI 5011, station 157.20). White = cartilage; stippled = ossifying.

plankton at a smaller size than the *Antennarius* species: although the *Antennatus* settlement size is unknown it certainly is <11 mm and probably near 5 mm. The *Antennarius* species settle at about 8 mm or a little larger.

A. avalonis has a specialized postflexion larval stage, the scutatus, that distinguishes it from the other two

species. The scutatus is characterized by large, postero-dorsal projections of the skull and a marked broadening of some bones of the suspensorium (fig. 11b; Pietsch 1984; Pietsch and Grobecker 1987). Watson (1996) erroneously stated that *A. sanguineus* also has a scutatus stage, based on the external appearance of the largest of the few lar-

vae then available. Additional specimens found later did not share this scutatus-like appearance, and clearing and staining clearly demonstrated that *A. sanguineus* does not have a scutatus stage. In scutatus stage *A. avalonis* > ca. 5 mm the posterior margins of the cranial extensions are outlined with melanophores (fig. 11a).

The presence of the specialized scutatus larval stage in *A. avalonis* and *A. radiosus* (Schultz 1957; Hubbs 1958; Pietsch 1984)—both members of the *A. ocellatus* species group (Pietsch and Grobecker 1987)—and the absence of a scutatus in *A. sanguineus*—a member of the *A. nummifer* species group (Pietsch and Grobecker 1987)—supports separation of these groups and suggests that the scutatus stage may be a unique specialization of the *ocellatus* group. The similar development of the dermal spinules in the two *Antennarius* species, and their different timing and mode of development in *Antennatus strigatus*, suggests that the ontogeny of dermal spinules, when better known, may provide insight into the questions of *Antennarius* monophyly and the interrelationships of the antennariid genera, which currently are largely unknown (Pietsch and Grobecker 1987).

ACKNOWLEDGMENTS

LITERATURE CITED

Hubbs, C. L. 1958. *Dikellorhynchus* and *Kanazawaichthys*: nominal fish genera interpreted as based on prejuveniles of *Malacanthus* and *Antennarius*, respectively. Copeia 1958 (4):282–285.

Kramer, D., M. J. Kalin, E. G. Stevens, J. R. Thrailkill, and J. R. Zweifel. 1972. Collecting and processing data on fish eggs and larvae in the California Current region. NOAA Tech. Rep. NMFS Circ. 370, 38 pp.

Moser, H. G. 1996. Introduction. *In* The early stages of fishes in the California Current region, H. G. Moser, ed. Calif. Coop. Oceanic Fish. Invest. Atlas 33, pp. 1–72.

Moser, H. G., E. H. Ahlstrom, D. Kramer, and E. G. Stevens. 1974. Distribution and abundance of fish eggs and larvae in the Gulf of California. Calif. Coop. Oceanic Fish. Invest. Rep. 17:112–128.

Moser, H. G., R. L. Charter, P. E. Smith, D. A. Ambrose, S. R. Charter, C. A. Meyer, E. M. Sandknop, and W. Watson. 1994. Distributional atlas of fish larvae in the California Current region: taxa with less than 1000 total larvae, 1951 through 1984. Calif. Coop. Oceanic Fish. Invest. Atlas 32, 181 pp.

Pietsch, T. W. 1981. The osteology and relationships of the anglerfish genus *Tetrabrachium* with comments on lophiiform classification. Fish. Bull., U.S. 79(3):387–419.

———. 1984. Lophiiformes: development and relationships. *In* Ontogeny and systematics of fishes, H. G. Moser, W. J. Richards, D. M. Cohen, M. P. Fahay, A. W. Kendall Jr., and S. L. Richardson, eds. Am. Soc. Ichthyol. Herpetol. Spec. Publ. No. 1, pp. 320–325.

Pietsch, T. W., and D. B. Grobecker. 1987. Frogfishes of the world. Systematics, zoogeography, and behavioral ecology. Stanford, Calif.: Stanford Univ. Press, 420 pp.

Schneider, M., and R. J. Lavenberg. 1995. Antennariidae. *In* Guia FAO para la identificacion de especies para los fines de la pesca. Pacifico Centro–Oriental, W. Fischer, F. Krupp, W. Schneider, C. Sommer, K. E. Carpenter, and V. H. Niem, eds. FAO Rome, pp. 854–857.

Schultz, L. P. 1957. The frogfishes of the family Antennariidae. Proc. U.S. Nat. Mus. 107(3383):47–105.

SIO. Scripps Institution of Oceanography. 1965. Oceanic observations of the Pacific: 1958. Berkeley: Univ. Calif. Press, 804 pp.

Taylor, W. R., and G. C. Van Dyke. 1985. Revised procedures for staining and clearing small fishes and other vertebrates for bone and cartilage study. Cybium 9(2):107–119.

Watson, W. 1996. Lophiiformes. *In* The early stages of fishes in the California Current region, H. G. Moser, ed. Calif. Coop. Oceanic Fish. Invest. Atlas 33, pp. 550–595.

APPENDIX. SPECIMENS USED FOR THE PREPARATION OF DESCRIPTIONS

Antennarius avalonis Jordan and Starks 1907

5 larvae: CalCOFI 5011, station 157.20 (1: 5.3 mm); IATTC 90037, station T-6 (1: 6.5 mm); IATTC 90043, station T-2 (1: 7.8 mm); IATTC 91001, station T-5 (1: 4.9 mm); IATTC 91005, station T-8 (1: 7.3 mm).

Antennarius sanguineus Gill 1863

13 larvae: CalCOFI 5209, station 152G.41 (1: 2.9 mm), station 153G.32 (1: 2.9 mm), station 157.20 (1: 5.1 mm); CalCOFI 5612, station 163G.30 (1: 6.7 mm), station 173G.10 (1: 3.2 mm); CalCOFI 5706, station 153.20 (1: 3.6 mm); CalCOFI 5708, station 106G.00 (1: 3.2 mm), station 145G.40 (1: 2.6 mm), station 151G.100 (1: 2.8 mm), station 157G.70 (2: 2.8, 8.4 mm); SIO Expedition Scot (TO 58-1), station 105 (1: 8.1 mm), station 137 (1: 8.1 mm).

35 juveniles: SIO 61-242 (6: 16.3–38.0 mm); SIO 62-55 (29: 8.1–29.0 mm).

Antennatus strigatus (Gill 1863)

4 larvae: CalCOFI 5708, station 145G.30 (1: 3.4 mm), station 145G.85 (1: 4.1 mm), station 151G.100 (1: 2.3 mm); IATTC 90048, station T-3 (1: 5.1 mm).

6 juveniles: SIO 59-225 (5: 10.9–14.2 mm); SIO 67-39 (1: 11.6 mm).